

# Instrumented Dynamic Penetrometers for Geotechnical Characterization

Pierre Breul<sup>1</sup>, Philippe Reiffsteck<sup>2</sup>

<sup>1</sup>*Institut Pascal, Université Clermont Auvergne, Clermont Auvergne INP, Aubière, France*

<sup>2</sup>*SRO, Université Gustave Eiffel, IFSTTAR, Marne la Vallée, France*

*Corresponding author: pierre.breul@uca.fr*

## ABSTRACT

The dynamic penetrometer is a common technique in geotechnical exploration and widely deployed throughout the world. However, while this technique has many advantages, it also has several disadvantages that can hinder its use and development. Indeed, it has evolved little, and its application has sometimes remained "rustic". But in recent years with the development of sensors, interpretation methods and digital technology, this technique has been adapted to improve the quality of measurement, the understanding of the phenomena occurring during the test and its exploitation. This article presents the recent developments and adaptations of this technique and their potential. After a brief review of the principle, history, and current limitations of the technique, we look at recent technological developments and the latest advances in terms of interpreting and using the test.

**Keywords:** Dynamic Penetrometer, instrumented DCP, soil characterization, in-situ test.

## 1. Introduction

Among the wide range of in situ geotechnical tests currently available (Mayne, 2006), dynamic penetration tests (DPT) are the most commonly used for soil characterization. Due to its rapid implementation, affordability and suitability for most soil types, DPT are present in current geotechnical practice in many countries around the world (Sanglerat, 1972). This is certainly the oldest one technique for geotechnical soil characterization. According to literature review presented by (Massarch, 2014), the first known experiences of the DPT date back to the 17<sup>th</sup> century in Europe. Generally speaking, a dynamic penetration test consists of driving a set of rods fitted with a conical tip (or in the case of Standard Penetration Test SPT, fitted with a sampler tube) into the ground and measuring the resistance of the soil to the driving action, as already specified by N. Goldman in 1699 (Goldmann, 1699). The use of such a device has the advantage of stressing the soil in its natural state of stress, and its ability to record soil resistance almost continuously is of great interest.

Nevertheless, the technique is not without faults and drawbacks, which sometimes limit its use or operating possibilities.

This article will review the history of this device and provide an overview of the different types of equipment and practice, while highlighting its limitations. In the second part, we present current developments aimed at improving it, particularly in terms of measurement.

Finally, we'll devote the last part to presenting recent improvements in its interpretation and operation.

## 2. History and current state of dynamic penetration

The idea of pushing rods into the ground to determine its resistance is a very old one. Indeed, in 1846 in France, Collin used a Vicat-type pocket penetrometer to estimate the cohesion of different types of clay (Sanglerat, 1972). However, the lack of precise specifications for the sizing of penetrometers has led to the development of a wide range of devices of all sizes.

### 2.1. Different type of equipment

The test consists of driving a set of metal rods or tubes, often fitted with a conical tip with a cross-section noted  $A_c$ , into the ground. Throughout the test, the number of blows  $N_x$  or the energy  $E$  required to drive the device into the ground to a given depth  $x$  is counted. While there are many different versions (Figure 1), generally speaking, a dynamic penetrometer comprises four main components (Figure 2) (Broms 1988):

- a ram, which generates energy by falling. The blow energy may or may not be constant.
- an anvil that transmits the energy to the rods. The contact between the anvil and the ram, as well as the connection between the anvil and the rods, are the most common places where energy is dissipated.
- a set of rods that transmits the beating energy to the tip in the form of a wave train. The wave train is reflected at the tip, transmitting part of its energy to the ground. Lateral friction between the rod train and the ground is not to be overlooked and can be the main cause of energy loss.
- a cone that punches into the ground, characterized by its diameter and the length of its shaft.

It should be noted that among dynamic penetrometer tests, the Standard Penetration Test (SPT) combines an in-situ measurement of soil resistance with a sample that enables precise identification of the soil to be tested precise identification of the soil to be tested.

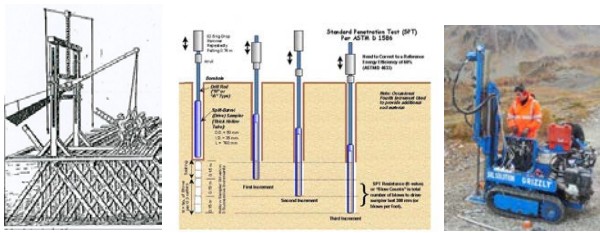


**Figure 1.** Different types of dynamic penetrometers a. Historical one b. SPT c. DPT.

## 2.2. Practices

If DPT is often considered simple to perform, its interpretation remains a complex subject once it involves the interactions of the hammer, anvil, rods, tip, and soil under the application of each blow performed during the test. A dynamic penetration test is often exploited by plotting a curve called penetrogram and providing the distribution of tip soil resistance ( $q_d$ ) as a function of depth. To obtain the tip soil resistance  $q_d$ , various calculation formulas are used, based on either from energy balance studies, or from the theory of wave propagation.

### a) Energy methods: beating formulas

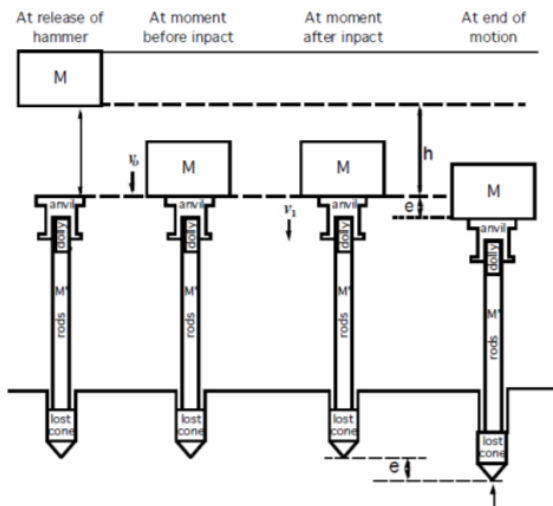


**Figure 2.** Illustration of the penetrometric beating phenomenon (Be 2011).

Beating or driving formulas usually applied to dynamic tests are based on a simple conservation energy principle. It consists in considering hammer energy before impact equal to work done by total resistance to driving plus different energy losses.

The general formula providing soil resistance from a dynamic penetrometer impact test is (eq. 1):

$$Q_d e = \frac{MgH}{(1+a)e} \frac{1}{\left(1 + \frac{c}{e}\right)} (1 + \varepsilon a) + (M + P)ge \quad (1)$$

With:

$a$  = the ratio between the mass of the body ( $P$ ) and the mass of the hammer ( $M$ );  $a = P/M$ .

$MgH / [(1+a).e]$  = soil resistance in the case of perfectly inelastic soil, with  $g$  the acceleration of gravity.

$e$  = the plastic displacement of the cone, tip penetration.  $c$  = correction factor.

$1 / (1 + c / e)$  = the dimensionless correction factor  $\leq 1$ .

This factor takes into account energy losses due to elastic deformation of the penetrometer and the soil.

$(1 + \varepsilon^2 a)$  = the dimensionless correction factor  $\leq 1$ , which takes into account the elasticity of the shock, with  $\varepsilon$  the Newton coefficient of restitution.

$H$  = drop height.

This general beating equation is obtained by applying Newton's shock theory and performing a pre- and post-impact energy balance. Several beating formulas are derived from the general equation, and assumptions are made to allow for energy losses of three types: elastic deformations of the penetrometer and soil, the inelastic nature of the shock and, in some cases, the resistance provided by water (Benz-Navarrete 2009).

Hiley's formula considers the case of a shock that is not perfectly inelastic ( $\varepsilon \neq 0$ ) and applies for elastic deformations of the penetrometer and soil of less than 10 mm, i.e.  $c < 0.5$ .

The Dutch formula considers a perfectly inelastic shock ( $\varepsilon = 0$ ) and negligible elastic deformations of the penetrometer and soil ( $c = 0$ ).

The Crandall formula considers a perfectly inelastic shock ( $\varepsilon = 0$ ), and non-negligible elastic deformations of the penetrometer and soil ( $c \neq 0$ ).

Despite these assumptions, at present, the Dutch formula is generally considered to give satisfactory results for small rod lengths and mass ratios. However, it should be noted that for low values of plastic embedment  $e$ , the dynamic resistance calculated by the Dutchman formula can reach very high values. Thus, when  $e < 5$  mm, formulas that take elastic deformations into account should be used. An alternative application of the Dutch formula recommended by EN ISO 22476-2 (2005) consists of replacing potential energy ( $MgH$ ) for actual transferred energy (EFV). The calculation of transferred energy relies on wave equation theory which is addressed in the next section.

### b) Wave Equation-based approach

One of the shortcomings of pile-driving formulas is that in most of the cases, the deformation of the penetrometer (or pile) is only treated in a highly simplified way or as a rigid body (Frank 1995). Moreover, these formulas assume the existence of a constant resistance during driving. These assumptions are far removed from the actual behavior of soils under dynamic loading. In fact, the impact of the ram on the anvil generates a train of waves that propagate with finite velocity through the set of rods (Isaacs 1931; Saint-Venant 1867). During dynamic test each hammer blow creates a compressional wave that propagates at speed  $c$  downward the rod, so that the time necessary for the wave to traverse the body becomes of practical importance.

Considering homogeneous elastic rod with uniform section if external forces (e.g. skin friction)

**Table 1.** Methods proposed to calculate soil resistance ( $q_d$ ) from dynamic penetration tests.

Approach	Method	Notation	Equation	Reference	Considerations
Newtonian	Dutch formula (DF)	$q_{d,DF}$	$q_{d,DF} = \frac{1}{A_t} \frac{MgH}{e} \frac{M}{(M+P)}$	(ISO 2005); (Sanglerat 1994)	Impact considered perfectly inelastic. Penetrometer and soil elastic deformations assumed negligible.
Newtonian/ Wave Equation	Dutch Formula with Energy Measurement (DF-EFV)	$q_{d,DF-EFV}$	$q_{d,DF} = \frac{1}{A_t} \frac{EFV}{e} \frac{M}{(M+P)}$	(ISO 2005)	Variation of DF in which potential energy is replaced by EFV.
Wave equation	Case Method (Case)	$q_{d,Case}$	$q_{d,Case} = \frac{1}{A_t} [F_A(t_1) + F_A(t_1 + 2L/c)] + \frac{2L}{A_t} [v_A(t_1) - v_A(t_1 + 2L/c)]$ Where $F_A(t)$ and $v_A(t)$ are force and velocity signals measured at point A in the pile head at the initial time $t_1$ often taken at the time when the force $F_A(t)$ is maximum.	(Rausche et al. 1985)	Pile assumed elastic, homogeneous and of uniform cross-sectional area. Impacts fully mobilizes the soil resistance in the shaft and at the tip. Plastic rigid soil-pile interaction is assumed (lateral friction and reaction under the tip are entirely mobilized at the arrival of the wave and remains constant).
Wave equation	Simplified Method (SM)	$q_{d,SM}$	$q_{d,SM} = \frac{1}{A_t} \left( \frac{EFV}{s_p + s_e} \right)$	(Paikowsky and Chernauskas 1992)	Maximum ( $s_{max}$ ) and final displacements ( $s_p$ ) after the impact are also determined from integration of velocity signal. Elastic displacement $s_e$ being the difference between $s_p$ and $s_{max}$ . In this study, the term $s_e/2$ is assumed negligible.
Wave equation	Unloading Point Method (UPM)	$q_{d,UPM}$	$q_{d,UPM} = \frac{1}{A_t} [Ks(t) + ma(t)]$ Where K is a spring constant, and m is the mass. The displacement, and acceleration expressed by $s(t)$ , and $a(t)$ respectively.	(Middendorp et al. 1992)	Resistance defined as the total resistance measured at moment when velocity is zero (time referred as $t_1$ ) when damping force are assumed equals zero. Inertial coefficient $m$ is neglected due to the low mass of penetrometer ( $m = 0$ ).
Wave equation	Tip Force Integration Method (TFIM)	$q_{d,TFIM}$	$q_{d,TFIM} = \frac{1}{A_t} \left( \frac{1}{s_{max}} \int_0^{s_{max}} F_t ds \right)$	(Tran et al. 2016)	Average resistance calculated directly from integration of tip force $F_t$ with integration interval between zero and $s_{max}$ . Force and displacement signals are estimated at the tip as described by (Benz Navarrete et al. 2021).

along the rods are negligible, propagation of the wave  $u(x,t)$  through the rod can be described by the so-called wave equation (eq. 2) (Saint-Venant 1867).

$$\frac{\partial^2 u(x, t)}{\partial t^2} = c^2 \frac{\partial^2 u(x, t)}{\partial x^2} \quad (2)$$

In the train of rods, these waves provoke a succession of sinking sequences corresponding to the rapid reciprocation of the rods in the penetrometer. The displacement of the penetrometer with each stroke takes place in several stages. Finally, the process stops when the tip stress falls below the soil plasticity threshold.

Based on wave equation analysis, several methods to determine cone resistance ( $q_d$ ) have arisen. One of the most popular methods is the Case Western Reserve University method (Goble et al. 1975) known as the Case method, which was originally proposed for driven piles applications. Other methods based on energy transmitted during the impact were proposed such as the Simplified Method (SM) (Paikowsky and Chernauskas 1992). The Unloading Point Method (UPM) was proposed by (Middendorp et al. 1986) for Statnamic pile tests analysis. Based on soil-pile interaction, this method defines the resistance as the total resistance measured at moment when velocity is zero and damping forces are not significant due to penetrometer small mass. More recently, using a specific wave analysis allowing tip signals assessment (Benz Navarrete et al. 2022), (Tran et al. 2016) proposed the Tip Force Integration Method (TFIM) to determine soil resistance.

Other works such as (Kianirad 2011; Kim et al. 2021) also propose to obtain soil resistance directly from force signal at the tip. The Table 1 summarizes different methods mentioned above, their formulation, notation, and main considerations.

### 2.3. Current limitations of the test

Although DPTs are very useful and convenient in practice, they provide only a single failure parameter: the blow count (N) or the dynamic cone resistance ( $q_d$ ). This value is not an intrinsic parameter of the soil, and its interpretation is still largely empirical. Indeed, to evaluate dynamic cone resistance, the pile driving formulae are usually employed (Lowery et al., 1968; Sanglerat, 1972; ISO-22476-2, 2005).

Similarly, the diversity of the beating or driving formulas used to process the measurements means that their interpretation is not straightforward and makes quantitative comparison between the various dynamic penetrometers highly imprecise and often disappointing. For example, the geometry of the tip and the scale ratio between the tip and the soil grains influence the results obtained. Indeed, in a given soil, tip resistance generally increases with decreasing tip diameter (Sanglerat 1972). Expressing DPT results in terms of cone resistance and not as a number of blows per penetration (e.g. N10, N20, 30) allows to compare and combine results from penetrometers of different sizes, i.e. Dynamic Probing Lightweight (DPL), Dynamic Probing Medium (DPM), Dynamic Probing Heavy (DPH) or Dynamic Probing Super-Heavy (DPSH) (Butcher et al. 1996).

In addition, the beating technique gives rise to various problems that need to be mastered or specified, so that the rate of energy delivered can be rigorously assessed and the penetrogram exploited. Indeed, studies show that energy losses can be obtained at the various interfaces of the tool parts and due to poor clamping between the shanks (Byun and Lee 2013).

Finally, interpreting the tip resistance remains a complex problem, as it includes initial and boundary conditions that are extremely difficult to model.

Nevertheless, numerous theories and works have been employed to provide answers. Experimental studies (on scale models, centrifuges or full-scale experiments) (Grésillon 1970), (Foray 1972), (Puech 1975), (Balachowski 1995) and (Emerson 2005) have described the evolution of the tip strength  $q_c$  as a function of depth, in the case of a homogeneous, pre-consolidated powder material, and have enabled us to distinguish the failure mechanisms around the peak observed at shallow depths from those observed at great depths.

Theoretical models of the initial penetration phase have been proposed, considering that the lateral displacement of the soil in the early stages of penetration can be represented by a bearing capacity model with an extension of the slip lines towards the soil surface (Yu and Mitchell 1998). Theoretical models have also been studied to analyze the evolution of peak resistance at depth, where penetration forces are governed by the compressibility of the soil and the increase in stresses around it. These approaches include cavity expansion theory, steady-state theory and numerical modeling.

In addition to energy determination and formula applied for cone resistance assessment, standard EN ISO 22476-2 (2005) gives some important recommendations concerning rods skin friction and groundwater table level. During dynamic tests, skin friction might develop along the rods which can result in overestimation of cone resistance. As suggested by EN ISO 22476 (2005), skin friction effect can be minimized using drilling mud during the test or torque measurements should be performed and used for data correction. Usually filling the annular space made by the cone enlargement with drilling mud is enough to prevent skin friction (Baudrillard 1974) when it is continually injected through hollow extension rods, just above where the cone is connected. The disadvantage of this solution is that it requires a special injection system (hollow rods and a pump) in addition to a water supply, which is not always available.

Therefore, several approaches were proposed aiming to correct rod skin friction in the post-treatment using torque measurements performed during the tests (Dahlberg and Bergdahl 1974; Mohammadi et al. 2012). Concerning the influence of pore pressure, depending on soil conditions, when the tip is moved, it is inevitable to produce a pore overpressure around the tip when penetrating saturated soils.

### 3. Technological developments

#### 3.1. Automatization

Various improvements have been made to the mechanical design of dynamic penetrometers. The aim has been to automate operations to make measurements more reliable and accurate. The GRIZZLY device (Benz-Navarrete et al. 2012) which is a fully automatic DPSH heavy penetrometer equipped with various sensors to automate in-situ measurements. The measuring principle is identical to that of conventional dynamic penetrometers. However, for each hammer impact, an automated digital procedure measures, calculates and records the penetration  $e$  and the peak resistance  $q_d$

calculated using the Dutch formula. To achieve this, the device is equipped with an impact counter that triggers the measurement of the depth of indentation using a robust, watertight, silent-block-mounted encoder to isolate any parasitic vibrations. The sensor's resolution is 50  $\mu\text{m}$ , ensuring an error of less than 1% over a depth of 10 m. Another sensor, located at the anvil, automatically detects the position of the pile driver (hammer) during drilling. It blocks the movement of the cylinders and the rods-driving process, ensuring that no parasitic load is applied to the rods during the lifting and lowering of the ram. The data is displayed in real time on the touch-screen, and at the end of the survey is stored and positioned using the integrated GPS.

(Chua and Lytton 1988) used the DPT in conjunction with an accelerometer mounted at the upper end of the device to analyse the dynamics of the penetrometer-soil system. Spectral analysis of the acceleration signal was performed to obtain soil damping parameters. The study shows that it is possible to estimate the hysteretic and viscous damping of soil in situ.

(Nazarian et al. 2000) instrumented a DPT with a load cell and accelerometer to measure the energy transferred to the anvil using the EFV method. In addition, a second device consisting of a three-dimensional accelerometer is introduced at the bottom of the hole to determine the modulus and Poisson's ratio of the layers traversed.

(Kianirad et al. 2011) has developed the Rapid Soil Characterization System (RapSoChS). This is a lightweight dynamic penetrometer equipped with various sensors to characterize surface soil properties. It combined electric cone penetrometer technology and a soil moisture sensor in a small pile-driving system similar to the DPT. The studies showed an acceptable estimate of cone resistance, lateral friction resistance and a ratio between these two values similar to the index given for the CPT.

#### 3.2. Energy Management

The first improvements made to dynamic penetrometers concerned the possibility of representing the phenomenon of penetrometric beating by the wave equation. (Schmertmann and Palacios 1979) were the first to measure wave propagation during penetrometric beating, in order to study the energy transmitted to the rods and the beating efficiency.

Later, numerous authors took an interest in the subject (Sy and Campanella 1991), (Aboumatar and Goble 1997), (Farrar 1998), (Daniel et al. 2005), (Odebrecht et al. 2005). Thus, it is common to find a corrective factor in the operation of tests that allows energy losses during beating to be taken into account. In practice, there are two main methods for measuring the energy transmitted to the stems: the EF2 method (Schmertmann and Palacios 1979) and the EFV method (Sy and Campanella 1991) (eq.3). These differ in the type and quantity of sensors used, as well as in the imposition of certain boundary conditions.

$$EF2(t) = \frac{c}{EA} \int_{t_0}^{t_0+2L/c} F(t)^2 dt \quad (3)$$

$$EFV(t) = \int_0^t F(t)v(t) dt$$

with  $c$  the wave velocity (m/s),  $E$  the Young's modulus (MPa) and  $A$  the rod cross-section (m<sup>2</sup>).

Although efforts have been made to improve the EF2 method (Matsumoto et al. 1992), work by (Benz-Navarrete 2009) has shown that the EFV method is best suited to penetrometric ramming. The efficiency of the driving system is expressed in terms of the CE coefficient, defined as the ratio between the energy transmitted to the stems by the impact and the theoretical impact energy (often  $M.g.h$ ). It has been shown that the CE coefficient depends not only on the impact system, but also on the length of the rods used (Figure 3) (Schmertmann and Palacios 1979); (Daniel et al. 2005). Today, in Europe as in the rest of the world, specifications (ASTM D 4633-10, NF EN ISO 22476-2) require frequent calibration of the impact energy of dynamic penetrometers. Numerous works were carried out to evaluate energy transmission in standard penetration test (SPT) and obtain the corrected NSPT number for an energy efficiency of 60% (N60) (Seed et al., 1985; Skempton, 1986; Sy and Campanella, 1991; Goble and Aboumatar, 1992, 1994; Aboumatar and Goble, 1997; Butler et al., 1998; Farrar, 1998; Farrar et al., 1998; Batilas et al., 2016).

(Byun and Lee 2013) have developed an instrumented dynamic cone penetrometer (IDCP) to assess the energy transferred in the cone tip. For this purpose, strain gauges and accelerometers were installed in the tip of the cone as well as in the upper end of the rod, below the anvil. The results show that the energy transferred to the tip of the penetrometer is significantly lower than that transferred to the head of the rod. This study suggests that energy losses caused by rod connections need to be taken into account, and that IDCP can be an interesting tool for characterizing steep locations.

(Gourvès 1991) and (Benz-Navarrete 2009) have applied these approaches to the Panda and Grizzly penetrometers, equipping the head of the device with various sensors (gauges and accelerometers) and thus making it possible to measure, in real time and for each impact of the hammer, the energy actually transmitted to the rods on the basis of the EFV method. It has been shown that the energy transmitted during hammering is not constant but is a function of the length of the set of rods (Figure 3).

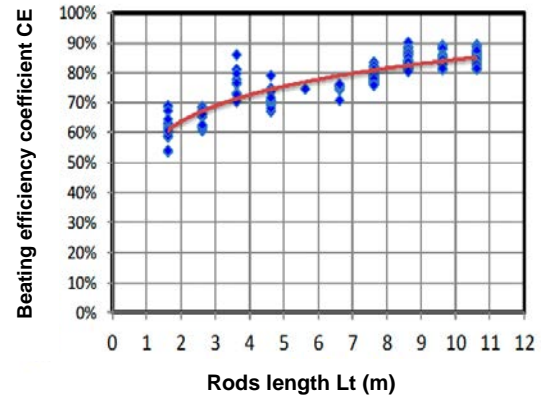


**Figure 3.** Evolution of the beating efficiency coefficient CE as function of the rod's length (Benz-Navarrete 2009).

Thus, for the GRIZZLY case, we can consider the following values for the driving efficiency coefficient CE ( $L_t$  = set of rods length):

- CE = 0,75 for a length  $L_t < 4$  m,
- CE = 0,8 for  $4 < L_t < 6$  m,
- CE = 0,85 for  $6 < L_t < 10$  m
- CE = 0,88 for  $L_t > 10$  m.

The corrections obtained are consistent with data reported in the literature and correlate well with those presented by (Morgano and Liang 1992). The values can be used to correct in situ and in real time the value of  $N$  or the indentation per blow measured during the test.

In practice, however, a lot of companies continue to count the number of blows (or the depth of penetration per blow) and use them for calculations without any correction of the value recorded in the field.

### 3.3. Variable Energy

One of the advantages of the dynamic penetration test is that it has a very high penetration power, enabling it to penetrate a wide range of soils. However, this advantage is also seen as a drawback when it comes to penetrating soft and/or saturated soils. In the latter case, the high penetration power can lead to interpretation bias (e.g., overestimation of cone resistance due to the creation of interstitial overpressures) or poor characterization of these layers due to the low number of measurements acquired.

To overcome these drawbacks, adaptive variable-energy driving systems have been developed in recent years. These consist in substituting the calibrated mass of the hammer with a striking mass whose drop height can be adapted, or with an unguided striking mass. In the latter case, test operation requires measurement of the energy supplied by the impacting mass, which can be done in a variety of ways (Figure 4). It is then possible to substitute the measured energy of the striking mass for the potential energy in the Dutchman's formula (Gourvès 1991).

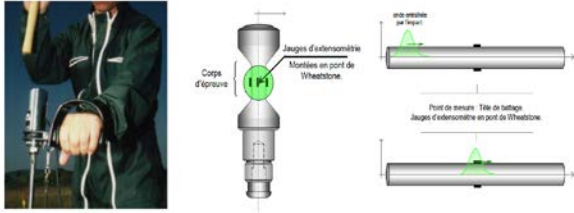


**Figure 4:** Example of variable energy provided by a hand hammer and sensors implemented on the anvil for measuring of the energy supplied by the impacting mass.

### 3.4. Signal Analysis (wave decoupling)

It is now well accepted that penetrometer driving is better represented by the wave equation solution. Isaacs (1931) and Smith (1962) suggested applying this theory for the study of concrete pile driving, and subsequently many authors worked on the numerical and practical implementation of the wave equation in order to improve the bearing capacity prediction of driven piles (Smith, 1962; Aussedat, 1970; Rausche, 1970; Rausche et al., 1971, 1972, 1985; Meunier, 1974; Goble et al., 1975, 1980; Gonin, 1979, 1996; Middendorp and Weele, 1986; Holeyman, 1992; Hussein and Goble, 2004).

Notwithstanding the analogy with driven piles, few studies have implemented the wave equation solution to improve the interpretation of DPT. Among the rare works, Aussedat (1970) in France was certainly the first, by means of a laboratory penetrometer, to obtain stress-strain relation of soil using wave equation and experimental measurements. Later, Chen (1991), Goble and Aboumatar (1992, 1994), and Liang and Sheng (1993) attempted to determine soil parameters with a laboratory instrumented penetrometer in order to improve the pile bearing capacity prediction by wave equation. Nazarian et al. (1998), Kianirad et al. (2011), and Byun and Lee (2013) instrumented lightweight dynamic penetrometers and applied the same approach to correct cone index value by energy transfer and evaluate the soil strength. Recently, Zar zojus et al. (2013) and Kelevi sius and Zar zojus (2016) instrumented a dynamic penetrometer super high (DPSH) (ISO-22476-2, 2005) with an accelerometer to improve penetration measurements and blow count. Some important works have applied wave equation theory to interpret dynamic penetration combining it to interaction models (Rausche et al. 1994; Salgado et al. 2015) and other analysis (Aussedat 1970; Schnaid et al. 2009). These interpretation methods often require either calibration or further information about soil parameters (e.g. soil's density, Poisson's ratio), which in practice is not always available. Indeed, these works have shown that wave equation application paves the way to a better understanding of soil reaction to dynamic penetration enabling to assess new information about soil behavior parameters.

However, none of these works has made it possible to improve systematically the technology associated with DPT either to implement new methods of measurements and analysis, or to obtain in situ soil stress and strain necessary for the most current geotechnical problems. Benz Navarrete (2009), (Benz Navarrete et al., 2013; Escobar Valencia, 2015) instrumented a lightweight

dynamic penetrometer with new sensors installed on the penetrometer's anvil and were able to measure the strain  $\varepsilon(x, t)$  and acceleration  $a(x, t)$  variations caused within the rods by the compressional wave created immediately after each hammer blow. The wave force,  $F(t)$ , is calculated from the measured strain  $\varepsilon(x, t)$  using Hooke's law. A displacement sensor connected to the instrumented anvil allows to measure simultaneously the cone penetration displacement  $s(t)$  per blow (Figure 4). As presented before, when the hammer, animated by a speed  $v_m$ , strikes the anvil, a compressional wave  $u(x,t)$  is generated in the rods and propagates at a constant velocity  $c$  towards the cone of the penetrometer. Afterwards, when  $u(x,t)$  reaches the cone/soil interface, a part of it is transmitted to the soil, causing its deformation. The second part of the wave is reflected upwards into the rods and travels to the top of the penetrometer, where a new downward wave reflection occurs. The phenomenon becomes thus cyclical during cone penetration. The wave  $u(x,t)$  propagation is described by Jean le Rond d'Alembert's equation, known

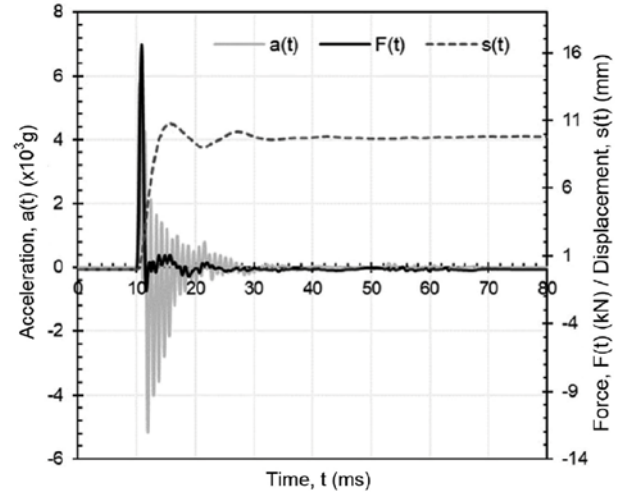


**Figure 4:** Example of a raw measurement of force  $F(t)$  (black line), acceleration  $a(t)$  (grey line) and displacement  $s(t)$  (grey dashed line) recorded for one blow during the penetrometer driving.

as the wave equation (eq.1).

Being for the case of the penetrometer a one-dimensional propagation phenomenon and according to the method of characteristics (Abbott, 1966; Middendorp and Weele, 1986; Verruijt, 2010), the general and most used solution to this equation is given by the overlap of downward  $u_f(x-ct)$  and upward  $u_g(x+ct)$  waves, where  $u_f$  and  $u_g$  are the arbitrary respective functions (eq. 4):

$$u(x, t) = u_f(x - ct) + u_g(x + ct) \quad (4)$$

Knowing the  $u_f$  and  $u_g$  waves at a point  $x_A$  in the rods, it is possible to determine for each  $x$  point along the rods, the stress  $\sigma(x,t)$ , strain  $\varepsilon(x, t)$ , velocity  $v(x, t)$  as well as displacement  $u(x, t)$ . In fact, for a plane wave and single mode propagation, stress, strain, velocity, and displacement can be expressed in terms of the Fourier transforms and as a function of these waves (eq. 5):

$$\begin{aligned}\tilde{\varepsilon}(x, \omega) &= A(\omega)e^{-i\xi(\omega)x} + B(\omega)e^{i\xi(\omega)x} \\ \tilde{\sigma}(x, \omega) &= E^*(\omega) \left[ A(\omega)e^{-i\xi(\omega)x} + B(\omega)e^{i\xi(\omega)x} \right] \\ \tilde{v}(x, \omega) &= \frac{\omega}{\xi(\omega)} \left[ A(\omega)e^{-i\xi(\omega)x} - B(\omega)e^{i\xi(\omega)x} \right] \quad (5) \\ \tilde{u}(x, \omega) &= \frac{i}{\xi(\omega)} \left[ A(\omega)e^{-i\xi(\omega)x} - B(\omega)e^{i\xi(\omega)x} \right]\end{aligned}$$

where  $A(\omega)$  and  $B(\omega)$  are the Fourier components of the downward  $u_f$  and upward  $u_g$  waves, respectively;  $E^*(\omega)$  is the complex Young's modulus; and  $\omega$  is the angular frequency. The wave number  $\xi(\omega)$  is a complex function defined by  $\xi(\omega) = k(\omega) + i\alpha(\omega)$ , where  $k$  and  $\alpha$  are the real and imaginary components. The two parameters,  $E^*(\omega)$  and  $\xi(\omega)$ , depend only on the rod characteristics, geometry and material (Bussac et al., 2002; Lodygowski and Rusinek, 2014; Othman, 2014).

The general problem is thus reduced to determine the Fourier components  $A(\omega)$  and  $B(\omega)$ , which is the same as determining  $u_f$  and  $u_g$  in the time domain from Eq. (4).

In practice, dynamic measurements during penetrometer driving can be performed by means of strain gauges and accelerometers. However, decoupling waves and the assessment of  $u_f$  and  $u_g$  components are not an easy task. This is because these waves are noisy and often superimposed in recorded signal, especially in the case of a penetrometer where steel and short rods are employed (wave velocity in steel is about 5200 m/s). Therefore, it is necessary to separate them by means of adapted and precise methods. Wave decoupling can be performed by different methods. These are distinguished on the types and number of sensors used as well as initial and boundary conditions. Without underestimating the signal processing methods developed during the last 30 years for pile dynamic test (Goble et al., 1980; Hussein and Goble, 2004; Middendorp and Verbeek, 2006), actually, the most precise and effective methods for wave decoupling and waveform calculation have been developed for rapid shocks tests, split Hopkinson pressure bar (SPHB) tests as well as solving percussion problems of rocks (Zhao and Gary, 1997; Park and Zhou, 1999; Bussac et al., 2002; Casem et al., 2003; Jung et al., 2006; Othman, 2014), as shown in Lodygowski and Rusinek (2014).

According to this method, if the geometry and the distance between impedance change planes are known, the stress and velocity at the lower extremity  $n$  can be calculated from previous measurement point ( $n-1$ ) where stress and velocity were known.

### 3.5. Independence from gravity

Another adaptation has been developed to make penetrometers independent of gravity, so that they can be used to test soils in hard-to-reach locations, or where the verticality of the penetrometer is difficult to ensure (slopes, cliffs, structures, etc.) (Figure 5). For this purpose, hydraulic driven hammer is replaced by a hand-held hammer. The energy supplied can be measured

directly after each impact in the penetrometer head or body.



Figure 5. Examples of non-vertical penetrometric tests

## 4. Recent advances in interpretation and exploitation

### 4.1. Compaction control

It has been shown that the cone resistance of a dynamic penetrometer test carried out in a well-known granular medium (particle size distribution and water content) is directly related to the dry density of the material (Jayawickrama, 2000; Livneh, 2013). Hence it is possible to establish a relationship between dry density and cone resistance for a material at given water content (Figure 6). Due to extreme sensitivity of cone resistance, the penetrogram is a signature of dry density variation and nature of the soil.

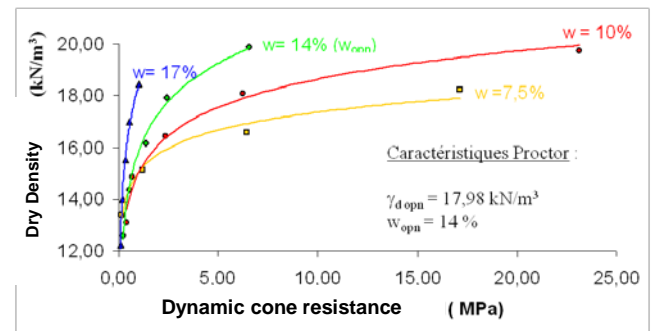
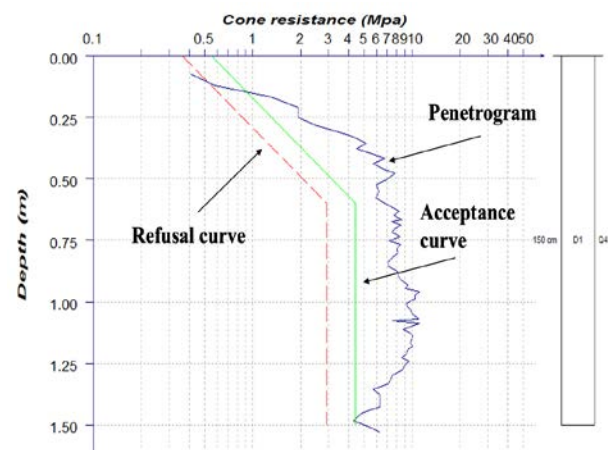


Figure 6: Relationship between dynamic cone resistance  $q_d$  and dry density for different water content.

Knowing these relationships for all types of soil representative of those used in backfill structures (relationships established on a laboratory soil database), it is possible to carry out automatic compaction control of these structures on site (Chaigneau, 2001).



**Figure 7.** Examples of a compaction test carried out with a penetrometer.

Once the penetrometer test has been carried out and the backfill structure has been defined (classification of materials used and required compaction level), the software superimposes the experimental penetrogram on the compaction acceptance and refusal curves for the materials tested (Figure 7).

#### 4.2. Load-bearing capacity and liquefaction analysis

The most popular investigation methods, such as the SPT, CPT and Ménard pressuremeter, have become popular with practitioners, not only because they provide reliable characterization of the subsoil (ground model, layering, derived parameters), but also because they have been supplemented by powerful tool kits for use in designing foundations, classifying soils and assessing liquefaction behaviour.

Rather than computing bearing capacity indirectly using Terzaghi relationship (Terzaghi and Peck, 1948) where parameters are often determined from in situ tests by empirical correlation which may be a major source of uncertainties. The direct design method has been preferred as based on the assumption of a similarity of the failure mechanism observed under the shallow foundation and during in situ test, propose a direct calculation using the equivalent resistance of the soil estimated using this test under foundation and the bearing capacity. The development of such methods depends on reliable database that bring together detailed test campaigns involving the loading of shallow foundations by dedicated structures. Numerous national research bodies and universities have undertaken parametric test campaigns on sites of various soil types and described by a detailed ground investigation campaign including dynamic penetration soundings. The formula used to calculate the net failure stress (bearing capacity per unit area) of a foundation subjected to a centered vertical load from the results of considered test is (eq. 6):

$$q_{net} = k_{test} \cdot \chi_c \quad (6)$$

with

- $q_{net}$  net stress,
- $k_{test}$  bearing capacity factor ( $k_d$  for DPT,  $k_c$  for CPT, etc.),
- $\chi_c$  equivalent resistance averages on 1.5 m.

In the case of dynamic penetration test, the average bearing factor  $k_d$  is observed to be equal to 0.225. The exact bearing capacity factor can be obtained using charts or empirical relationships (Figure 8). The curve number depends of soil category and shape of the footing.

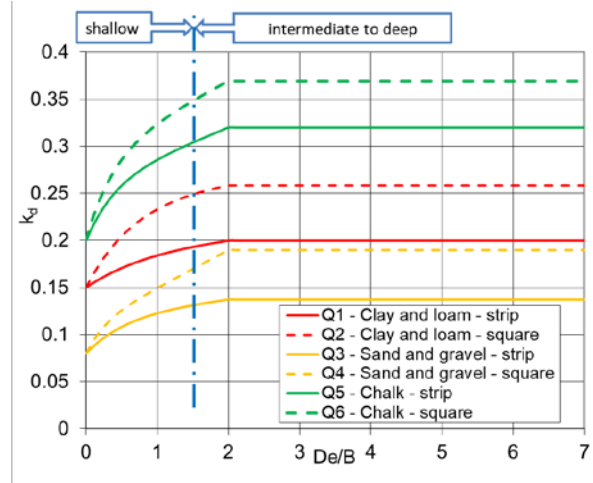


**Figure 8.** Effect of embedment for the different soils for the dynamic penetrometer method (Luong et al, 2024a)

In the case of a water table at depth in sand, we consider that during a penetration test in moderately compact sand, a "liquefaction" phenomenon (thixotropy) may occur which affects the dynamic resistance of the soil (sensitivity coefficient,  $s_L=2$ ). So for any test under the water table and in sand, we take (eq. 7):

$$q_d = q_{d\ test} \cdot s_L \quad (7)$$

The dispersion of the dynamic penetrometer bearing factor  $k_d$  is similar to that observed for the bearing factor defined for the CPT or PMT test (Figure 9).

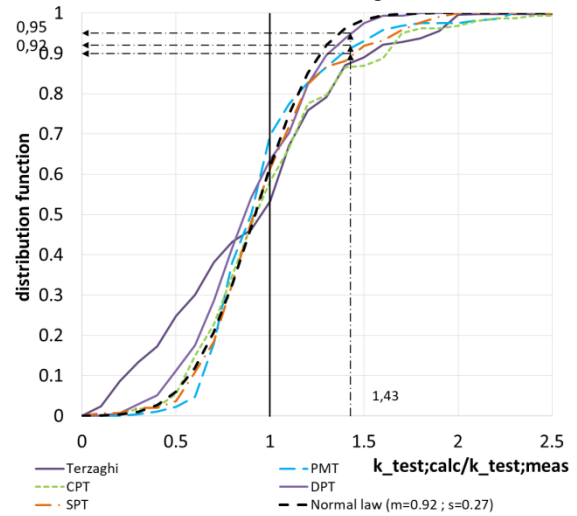


**Figure 9.** Relationship between dynamic cone resistance  $q_d$  and dry density for different water content (Luong et al, 2024b).

(Retamales et al, 2020) have recently develop a method of studying the risk of liquefaction proposed for dynamic penetrometers, applied to Panda 3® and Grizzly 3® measurements. A parametric study studied the evolution of cone resistance in two reference sands (Fontainebleau and Hostun) reconstituted sand beds, at different density index in a "K<sub>0</sub>" calibration chamber Retamales (2022). A good correlation is established between the dynamic cone resistance ( $q_d$ ) and the soil density index ( $I_d$ ) (Figure 10), allowing to apply the liquefaction risk study method proposed by Jara (2013) on in situ measurements with Panda 3® and Grizzly 3®

on a sandy site in southern France and to compare the results obtained with piezocone measurements (CPTu) according to Robertson and Wride (1998) method reported by Youd and Idriss (NCEER) to the static penetrometer (CPTu).

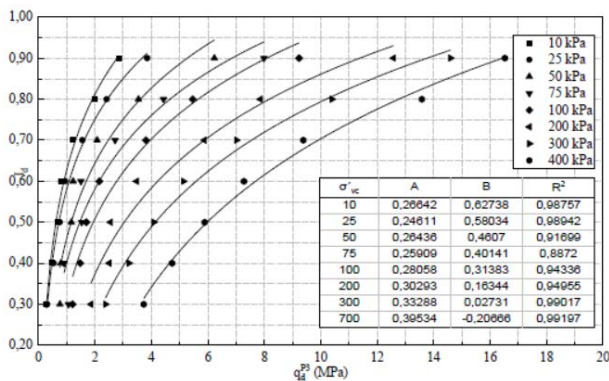


**Figure 10.** Relationship  $q_d^{p3} - I_d$  under different conditions of vertical confinement.

The use of lighter, less expensive equipment can be a significant advantage for assessing this risk in areas subject to seismic regulations. The obtained from the Panda 3® and Grizzly 3® are in good agreement with the results with the results measured using the traditional CPTu method.

Recently Luong et al. 2023 has applied this method along the Kupa, Sava and Glina rivers (Croatia) in Quaternary alluvial sediments where numerous liquefied sand ejections came to the surface during the Petrinja earthquake sequence in December 2020. It has emphasized the Panda's and Grizzly's ability to see the different layers recognized by geophysical and geological surveys and allow to correlate them to define a first geotechnical model and localize the soil unit sources of liquefaction and finally confirm the pertinence of the ground model obtained by both methods.

Comparison to other method based on shear wave velocities measured with cross-hole tests with the wave shear velocity measurements deduced from the Panda Panda 3® and Grizzly 3® tests is an ongoing development.

### 4.3. Load-displacement blow curve analysis

As previously demonstrated, by instrumenting a penetrometer and using the wave decoupling method, it is possible to reconstruct the signal at the tip of the penetrometer. Once the stress  $\sigma_I(t)$  and velocity  $v_I(t)$  signals are calculated for the penetrometer cone, strain  $\epsilon_I(t)$  and force  $F_I(t)$  are calculated by means of elasticity relationships presented in eq. (5). Displacement  $u_I(t)$  can be also calculated thought numerical integration of velocity  $v_I(t)$ .

By this means, and assuming that there is equal stress and displacement at the cone/soil interface during cone penetration, it is possible, after each blow, to provide a dynamic cone load-penetration (DCLT) curve (Figure 11). Theoretical, numerical as well as practical reliability of these method has been demonstrated recently by Benz Navarrete et al. (2013), Escobar Valencia et al. (2013,

2016a, b), Tran et al. (2017, 2019), and Zhang et al. (2019).

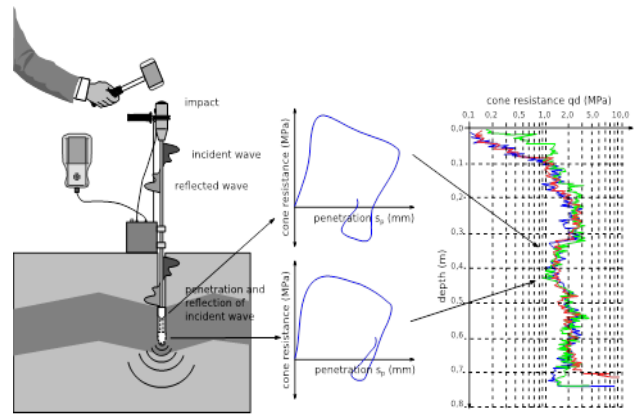


**Figure 11.** Dynamic cone load-penetration (DCLT) curve.

An analytical methodology is used to analyze this curve and to estimate additional strength and deformation parameters of the soil: dynamic and pseudo-static cone resistances, deformation modulus and wave velocity.

To assess soil mechanical impedance, wave velocity as well as strain, the shock polar curve method is applied (Figure 12) (Aussedat, 1970; Meunier, 1974; Oularbi, 1989; Oularbi and Levacher, 2009; Lodygowski and Rusinek, 2014; Omidvar et al., 2014; Iskander et al., 2015; Tran et al., 2019).

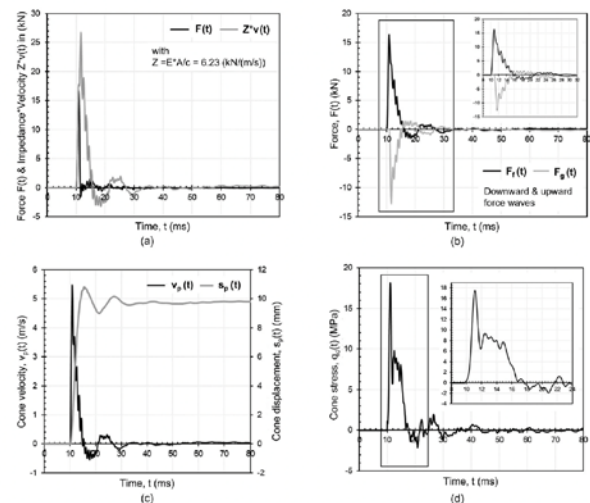


**Figure 12.** Example of dynamic measurement during penetrometer driving for Allier sand in a dense state: (a) Signals of force (black line) and velocity (grey line) multiplied by rod mechanical impedance  $Z$ . EA/c recorded at the measurement point  $x_A$  in the instrumented anvil of the device, (b) Decoupled forces of upward (grey line) and downward (black line) waves travelling into the rods after the blow, (c) Calculated cone signals for velocity  $v_p(t)$  (black line) and displacement  $s_p(t)$  (grey line), and (d) Calculated stress signal at the cone of the penetrometer with a zoom view between 8 ms and 24 ms.

The polar shock curve represents the relationship between stress ( $s$ ) and particular velocity ( $v$ ) generated by the mechanical wave which propagates in a defined material. In this method, it is assumed that a plane and unidirectional elastic shock wave propagates from a

medium A (rods) to a medium B (soil). By applying the shock polar curve method, it is possible to the DCLT curve of the material crossed. As shown on figure 13, a good repeatability of the curves obtained can be observed as well as its sensitivity to the type of material tested.

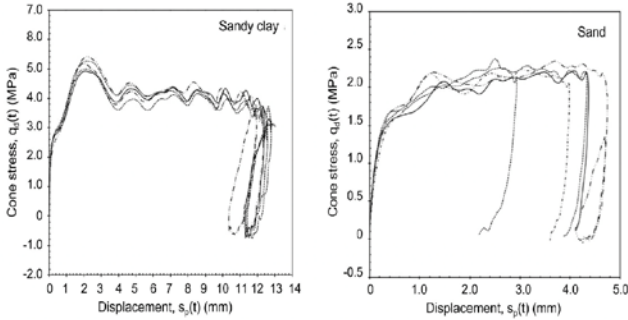


**Figure 13.** DCLT curves obtained from decoupled waves and cone signal calculation method on (a) sandy clay and (b) sand. For each graph, each curve represents an analysed blow.

From the results obtained for natural sandy clay, performed with a constant driving energy, where a very good repeatability can be observed, the curves obtained are almost identical for each blow. Concerning the curves obtained for sand at variable driving energy, it can be noted that the cone load increases proportionally to the displacement, following a nonlinear trend, as usually observed on base load-displacement response of piles in sand. It can also be observed that a maximum soil penetration resistance remains almost constant for each blow independently of driving energy, while total penetration increases proportionally. In addition, for driving energy employed here to obtain sand's DCLT curves, no significant rate effects on cone resistance were observed in our experiences, such as found in other similar experimental cases (Eiksund and Nordal, 1996).

For the case of soils, once cone resistance  $q_d(t)$  reaches a threshold value (close to the maximum stress), the soil deforms plastically and the cone resistance  $q_d(t)$  remains almost constant until the maximum penetration is reached. At this moment, the energy contained in the waves propagating inside the rods is not enough to continue deforming the soil and the unloading phase begins. After, a series of unloading and reloading cycles can be observed in some cases. Besides applying the Aussedat (1970)'s method, a simple analytical method was proposed to analyze DCLT curves obtained during penetrometer driving, as shown in Figure 14, based on simplified pile model (Benz Navarrete, 2009; Benz Navarrete et al., 2013, 2014; Escobar Valencia, 2015; Escobar Valencia et al., 2016b).

**Figure 14.** Interpretation of DCLT curve based on the simple Smith (1960)'s pile model: (a) General model represented by an elasto-viscoplastic model, and (b) Unloading/reloading zoom area.

The experimental DCLT curves can be separated into three phases (Figure. 14a): full dynamic penetration, plastic shear penetration and unloading/reloading cycles. Full dynamic penetration is mainly inertial and penetration rate dependent, while plastic shear penetration is penetration rate and displacement dependent. The unloading/reloading cycle, which follows the moment when the rate penetration becomes zero (at this moment, represented by the point A in Figure 14, the energy to penetrate the soil is not enough), is mainly elastic displacement dependent. The DCLT is modelled as a simplistic elasto-viscoplastic model (Figure 14a). Here, the total soil resistance  $q_d(t)$  is modelled with both viscous dynamic ( $q_{dyn}$ ) and pseudo-static ( $q_s$ ) components (Eq. 8). The total soil resistance is thus the sum of the spring reaction ( $q_s$ ) and the radiation dashpot reaction ( $q_{dyn}$ ) (Salgado et al., 2015).

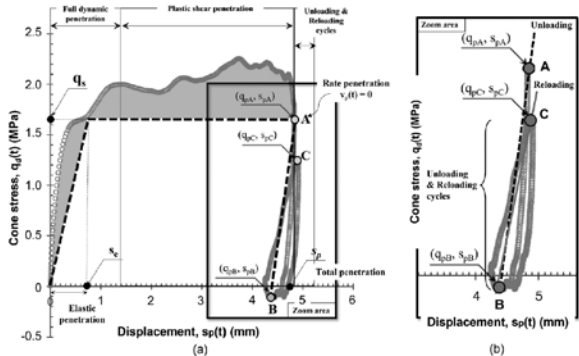
$$q_d(t) = q_s + q_{dyn} \quad (8)$$

$$q_s = q_d(t_A) \forall t = t_A \text{ when } v_p(t_A) \approx 0 \text{ and } s_p(t_A) = s_p \quad (9)$$

$$q_{dyn} = \frac{1}{s_p - s_e} \int_{s_e}^{s_p} [q_d(t) - q_s] ds \quad (10)$$

These two components can be separated from each DCLT curve. Pseudo-static resistance  $q_s$  is displacement dependent and then independent of penetration rate. This is modelled by an elastic perfectly plastic law and determined experimentally when average penetration rate is zero (Eq. 9). Knowing pseudo-static resistance value, viscous dynamic resistance ( $q_{dyn}$ ) is determined from dynamic loading curves as the average resistance mobilised in the penetration interval between elastic settlement  $s_e$  and maximum measured plastic penetration  $s_p$  once pseudo-static resistance is subtracted (Eq. 10).

From unloading and reloading cycles (slopes AB and BC, respectively, in Figure 14), dynamic elastic modulus  $E_{p3}$  can be determined. Once the maximum plastic penetration  $s_p$  is reached, the soil and penetrometer vibrate together in a pseudo-elastic steady state. Here, two moduli are defined: unloading modulus  $E_{dp3}$  and reloading modulus  $E_{rp3}$  (Eq. 11) Indeed, supposing that the cone penetrometer is a small circular plate embedded in a semi-infinite elastic medium,  $E_{dp3}$  and  $E_{rp3}$  values can be calculated from Boussinesq and Mindlin approaches (Arbaoui et al., 2006; Ali et al., 2008, 2009; Reiffsteck et al., 2008, 2009).



$$\left. \begin{aligned} E_{p3}^d &= (1 - \nu^2) \left( \frac{q_{pA} - q_{pB}}{s_{pA} - s_{pB}} \right) \frac{\pi d_p^2}{4} \frac{1}{k_M} \\ E_{p3}^r &= (1 - \nu^2) \left( \frac{q_{pA} - q_{pB}}{s_{pA} - s_{pB}} \right) \frac{\pi d_p^2}{4} \frac{1}{k_M} \end{aligned} \right\} \quad (11)$$

where  $n$  is the Poisson's ratio of the soil,  $d_p$  is the cone diameter, and  $k_M$  is the embedding Mindlin's coefficient.

To summarize, in practice, at the end of the dynamic penetration test according to the method presented, the following log profiles were produced: dynamic and pseudo-static cone resistance, unloading and reloading moduli, and compressional wave velocity. Shear wave velocity can be also determined by assuming the Poisson's ratio of the soil (Figure 15).

As previously stated, considering dynamic compression as well as undrained condition, Poisson's ratio will be close to 0.5.

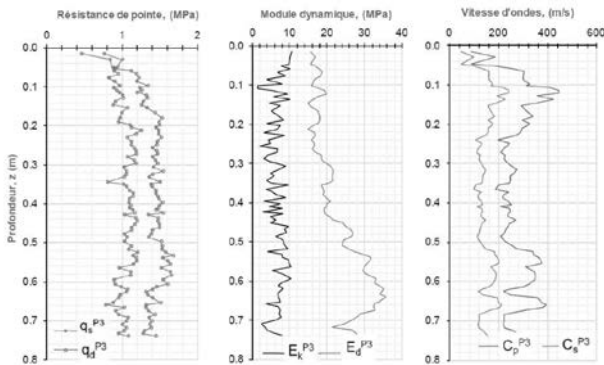


**Figure 15.** Log profiles obtained from the DCLT curves analysis: (a) tip resistance  $q_a$  et  $q_c$ , (b) dynamic stiffness  $E_{kDP3}$  and deformation modulus  $E_{dDP3}$ , (c) the shear and compressional waves celerity  $V_{sP3}$  et  $V_{pP3}$ .

#### 4.4. Modelling – behaviour in the neighbourhood of the tip and DPT interpretation

A great deal of numerical modelling work has been carried out in recent years to complement experimental developments, with a view to gaining a better understanding of the local phenomena occurring around the penetrometer tip during dynamic indentation/displacement (Sadr Abadi, 2016), or to better interpret the test (Foretti Oliveira 2022, Tran et al., 2016, 2017, 2018, 2019; Zhang, 2019) and the load-displacement curve obtained during the test, or to calibrate methods for characterizing granular media (Quezada, 2014; Schnaid et al. 2007, 2017).

Most of these works are based on the discrete element (DEM) or finite difference (FEM) method.

For example, Tran (2018) proposed a spectral analysis on dynamic cone penetration tests results, modelled with Discrete Element Method in order to assess the effect of the variation of the grain size distribution of the soil on test results. For each impact of the hammer, a curve of the load applied by the tip on the soil is obtained versus the penetration distance of the tip (Figure 16a). The curves of the load vs. penetration traditionally used to calculate the tip resistance of the soil, are analyzed with Discrete Fourier transform in order to investigate curve's shape. The effect of the variation of the grain size distribution of the soil on these curves is investigated (Figure 16b). It was found out that the grain size distribution influences tip resistance but also the shape and oscillation modes of the curve of the stress-penetration curve. Based on these indicators, the

exploitation of the load-displacement curve obtained with dynamic penetration tests could be enlarged to determine other properties of the soils.

A three-dimensional numerical model of the penetration test using the discrete element method (DEM) was also developed to reproduce the process of the test and validate the calculation method based on the decoupling of the ascending and descending compression waves that travel along the rod of the penetrometer and verify whether the behavior of the soil, i.e., at the tip, could be effectively and accurately calculated from the data recorded at the top of the device. The results showed

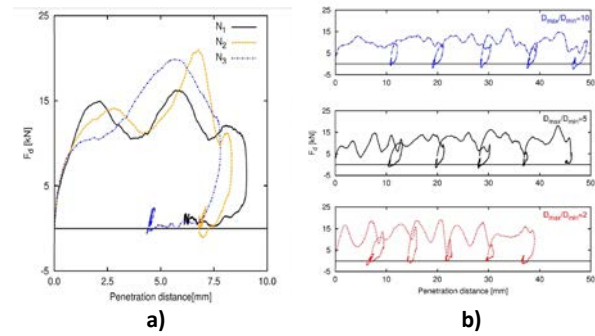


**Figure 16.** a) Example of load-penetration curves obtained in a dynamic cone penetration test for 3 impacts in material A - b) Tip force as a function of penetration distance for 5 successive dynamic penetration tests for 3 materials A, D and E.

a good correspondence between the calculated curve and the one observed at the tip (Figure 17); the order of magnitude of the stresses was the same, the major oscillations of the curve were observed at the same moment, and the part representing the unloading was also very accurate.

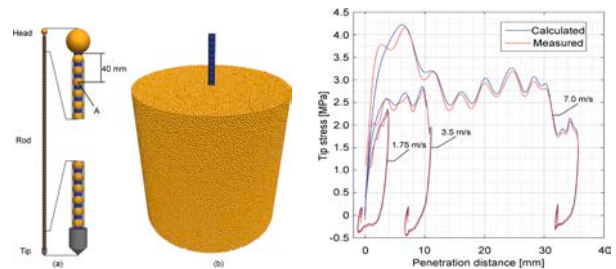


**Figure 17.** Numerical model: (a) view of the model representing the penetration test device, based on the Panda 3 specifications, and (b) view of the penetrometer driven in a sample of spheres. Comparison of the stress between the tip and the soil for impact velocities of 1.75, 3.5, and 7.0 m.s<sup>-1</sup>, obtained by the wave separation method (blue line) and actually observed at the tip of penetrometer (red line).

Foretti Oliveira (2022) investigates by using DF method if a simple approach based on driving formulas derived from Newtonian approach, such as Dutch Formula (DF), combined with good practice (e.g. energy measurement, skin friction control) can produce satisfactory results. Results showed that for shallow unsaturated layers, on average DF results were comparable to those from wave equation methods and to Cone Penetration Test (CPT) resistance. Wave equation methods results were comparable to CPT cone resistance in most cases.

Quezada (2014) studied the response of a dynamic penetration test in a coarse granular media where the physical interpretation of the output data is less obvious. Indeed, the data are considerably more sensitive in this case to various parameters such as fabric structure, particle shapes or the applied impact energy. A numerical study was performed by means of contact dynamics simulations. The dynamic penetration test in a sample composed of irregular grain shapes was studied and the influence of the driving velocity and input energy on the penetration strength was analyzed (Figure 18). The results show that the latter grows with both the penetration rate and energy, despite the strong fluctuations occur due to a jamming–unjamming process in which the contact network connectivity evolves intermittently in correlation with the penetration strength. This analysis suggests that the time-averaged data provided by a penetrometer is reliable information from which the bulk strength properties of coarse granular materials can be evaluated.

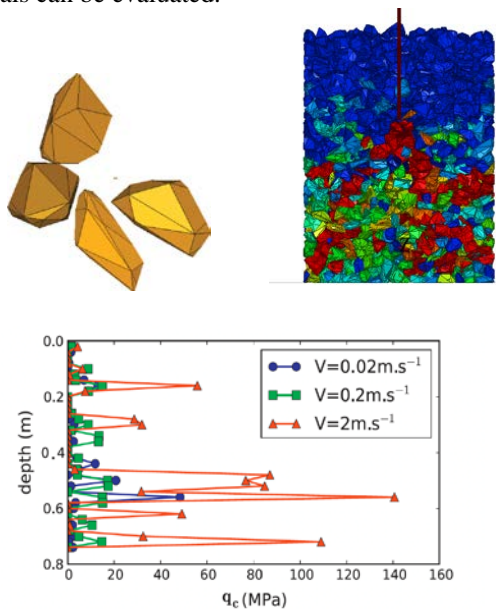


**Figure 18.** a) Four examples of polyhedral particles used in the simulations. b) Simulation of the dynamic penetration test in coarse material c) Penetrogram for several penetration rates, taking the values: 0.02, 0.2 and 2m.s<sup>-1</sup>.

#### 4.5. Statistical tools and AI for soil reconnaissance

Any geotechnical engineering project firstly requires the development of a conceptual ground model based on the soil data obtained from a site exploration program. This model is a synthetic and simplified representation of subsoil that contains the information on all strata, including their geometry, physical properties, and strength and deformation characteristics. However, these properties are certain only at the location where the measurements were performed. At other locations, they must be deduced from available data, in most cases reduced and widely spaced. The cognitive processes used in the ground model definition are fundamentally subjective, based on judgement and geotechnical expertise. Thus, the development of methodologies to

define a conceptual ground model in a more rigorous and systematic way, is a major challenge for current practice. Since the amount of available soil data is usually weak, especially for small or medium projects, it is difficult to produce meaningful statistics for subsequent geotechnical design and analysis. Therefore, current practice often relies on defining deterministic 1D soil models through basic statistical analysis and expert judgment. However, more realistic and reliable soil models must incorporate spatial soil variability and consider other soil uncertainties encountered during site characterisation. The dynamic penetration test can provide continuous soil measurements in a very rapid and economical manner. In this respect, propose a comprehensive probabilistic site characterization methodology based on the statistical interpretation of the dynamic cone resistance profiles is an ambitious goal.

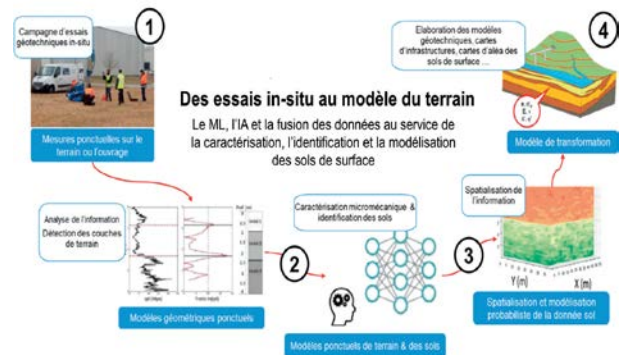


**Figure 19.** Overview of the proposed approach.

The proposed approach (Sastre 2018, Sastre et al. 2016, 2020, 2021) involves 4 main stages, shown in Figure 19. Following the soil investigation based on dynamic penetration tests (Figure 20), the first step deals with the Data acquisition — Machine learning algorithms and statistical analysis require many data that are as representative as possible for the problem to be addressed. The first phase is therefore to collect the data to create a data bank.

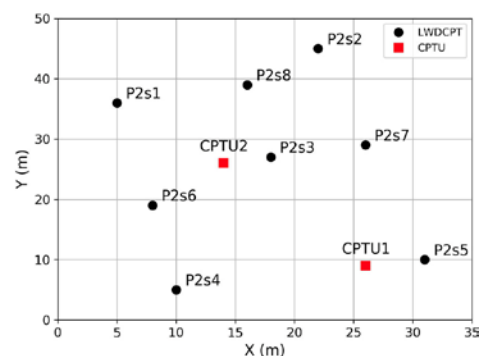


**Figure 20.** Relative location of LWDCPT and CPTU soundings.

The second step deals with the identification of underground soil stratification using a statistical moving window procedure to detect boundaries between mechanical homogeneous soil units. The third step release on the implementation of an automatic classification method based on artificial neuron networks (ANN) for estimating the nature of the soil crossed from the analysis of penetrometric signals. The last involves

spatial variability modelling through an anisotropic 3D random field and to build the ground model.

Concerning the automatic identification of underground soil stratification (step 2), the methodology proposed rests on the use of a moving window of a fixed width  $W_d$  to determine layer boundary location of the homogeneous units (assessed in terms of the mechanical response of soil to dynamic cone penetration rather than soil nature) (Figure 21). The center point of the window defines two sets of data (one above and one below). The two data samples are analyzed for distinctness using the  $T_{ratio}$  method (Wickremesinghe and Campanella 1991) which calculates t-Student's statistics as a sensitive test of the boundary position. For comparing two samples, statistics to compute  $T_{ratio}$  are calculated from data points lying within each segment. The window is moved along the profile in steps equal to the measurement sampling interval. We obtain a curve which draws the evolution of the parameter  $T_{ratio}$  according to the depth where the local maxima (peaks of the profile) give the optimal soil boundaries location. A given threshold value is used to identify local maxima representing soil layer boundaries.

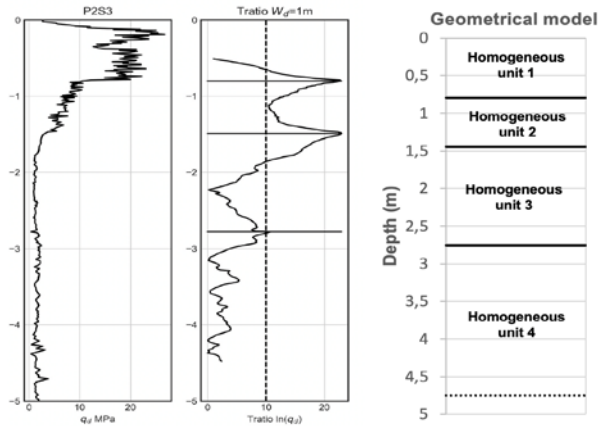


**Figure 21.** Identification of soil boundaries from P2S3 test using  $T_{ratio}$ .

Concerning the implementation of an automatic soil classification method based on artificial neuron networks (ANN), the method rests on different stages (Figure 22):

- Soil data base creation,
- Model input data definition to identify a vector of input variables representative of the objects to be classified regarding the classification problem to be addressed. By applying different signal analyses to the penetrogram, the goal is to detect parameters that will identify the penetration test with respect to the classification system. The aim is to create an intelligent associative memory by means of ANN between penetrograms and soil classes to be defined.
- Definition of model outputs - The next step is to set criteria based on the reference geotechnical classifications used in practice to define the number of model classes to be developed.
- System learning - This phase consists in training the network by means of the database developed.

The spatial variability modelling comprises the following steps.

- Applying the natural logarithm transformation to  $q_d$  data. Then, determining the average depth trend over all profiles available by performing a global regression.
- Transform the profiles into a standard normal field ( $\mu = 0$ ;  $\sigma = 1$ ).
- The scale of fluctuation is estimated from the transformed data separately in the vertical and horizontal direction. Vertically, the correlation function is estimated for each penetration test. Horizontally, horizontal correlation function is calculated by averaging each horizontal correlation function with respect to depth for

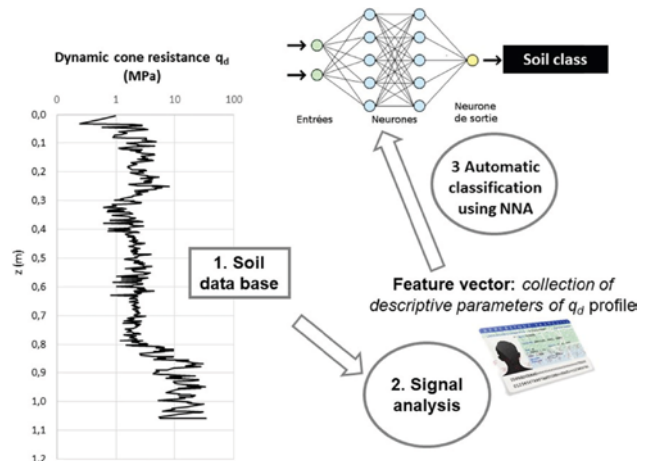


**Figure 22.** Diagram of proposed methodology for automatic soil classification

each homogeneous unit. Finally, the best fitting exponential model to the averaged empirical correlation function to estimate the vertical,  $\theta_v$ , and horizontal,  $\theta_H$ , scales of fluctuation is found.

(d) Obtaining an unconditional simulation  $V_U(X)$ , simulating a standard normal random field using the correlation model and the input parameters  $\theta_v$ ,  $\theta_H$  deduced in step c). This step may be repeated  $n$  times, where  $n$  is the total number of simulations to reach.

(e) Constraining the unconditional simulation generated in step d) at the test locations  $X_i$  (conditioning points). Firstly, the best estimate of the field is calculated by kriging the field,  $V_K(X)$ , using the conditioning points. Then, values at conditioning points  $X_i$  in the unconditional simulation  $V_U(X)$  generated in step d) are used to krig the simulated field to obtain  $V_S(X)$  (this operation may be repeated  $n$  times).

(f) Applying the inverse transformation procedure to obtain the  $q_d$  random field (Figure 23).

The left side of Figure 23 shows a 3D view of one possible realization of the conditional random field. On the right side of the same figure, we present two possible random soil profiles generated at the same locations of the two dynamic cone penetration tests used for validation purposes. The simulated soil profiles appear to be quite similar in a statistical sense, when compared with the real in-situ measurements.

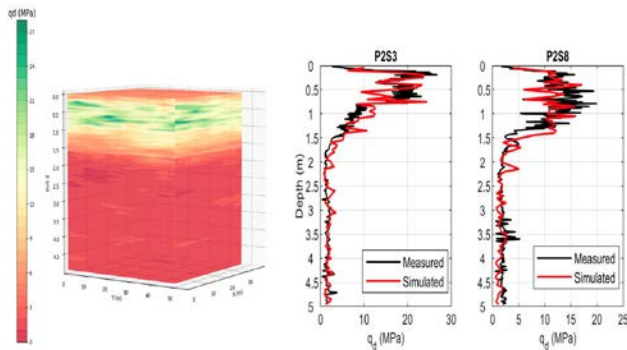


**Figure 23.** 3D Conditional random simulations and simulated against measured  $q_d$  profiles at the same location.

## 5. Conclusions

DPTs are widely used around the world and currently provide a single failure parameter whose interpretation is still largely empirical. Various improvements have been made to the mechanical design of the equipment. The aim has been to automate operations to make measurements more reliable and accurate (automatization, energy management...). Several authors proposed to improve the interpretation of the DPT by using the wave equation. Until recently, none of these works have been implemented in practice to obtain in situ soil stress and strain relationship necessary for the most current geotechnical problems.

As demonstrated, by using a monitored/instrumented penetrometer to measure the strain  $\epsilon(x, t)$ , acceleration  $a(x, t)$  and displacement  $s(t)$  variations caused within the rods by the compressional wave created immediately after each hammer blow and during penetrometer driving and by using a wave decoupling and reconstruction method, it is possible to obtain the DCLT curve of the soil at each blow. This DCLT curve is reproducible, sensitive, and reliable to the test conditions as well as to the soil conditions. Moreover, the implementation of the method based on a linear viscoelastic model and the Smith (1960) approach makes it possible to compute total, dynamic and pseudo-static soil resistances as well as the deformability moduli from DCLT curve. Finally, the application of the method proposed by Aussedat (1970) makes it possible to determine the soil impedance or shock polar curve, from which the soil compressional wave velocity can be calculated.

Despite the results obtained, the soil behaviour subjected to dynamic cone penetration remains poorly understood. Indeed, this is a nonhomogeneous loading test, and given its nonlinearity, the soil behaviour after blow is complex. This is why interpretation of the DCLT curve is a complex matter and is the subject of research to improve its understanding, and to develop methods (with the help of numerical modeling) in order to estimate intrinsic soil parameters governing stress-strain behaviour under dynamic penetration. Quantitative interpretation of dynamic penetrometers via wave analyses is particularly difficult in soft saturated soils, where the interpreted values are likely to be overestimated and should be carefully considered. But the high vertical resolution of the penetrometric test and its easy implementation also opens up new prospects for

soil analysis and interpretation using artificial intelligence and machine learning.

## 6. References

- Abbott, M.B., 1966. An introduction to the method of characteristics. In: *Finite Difference Methods in Financial Engineering: A Partial Differential Equation Approach*. Cambridge University Press, Cambridge, UK, pp. 47-59.
- Abou-matar, H., and G. Goble. 1997. "SPT Dynamic Analysis and Measurements." *Journal of Geotechnical and Geoenvironmental Engineering* 123 (10): 921-28. doi:10.1061/(ASCE)1090-0241(1997)123:10(921).
- AFNOR. (2012). *NF P 94-105 - Sols : Reconnaissance et Essais - Contrôle de La Qualité Du Compactage - Méthode Au Pénétrömètre Dynamique À Énergie Variable - Principe et Méthode D'étalonnage Du Pénétrömètre - Exploitation Des Résultats - Interprétation*.
- Ali, H., Reiffsteck, P., Bacconnet, C., Gourvès, R., Baguelin, F., van de Graaf, H., 2008. Facteurs d'influence de l'essai de chargement de pointe. Nantes, France. In: *Journées Natl. Géotechnique Géologie l'Ingénieur JNGG'08*, pp. 467-474 (in French).
- Ali, H., Reiffsteck, P., van de Graaf, H., van de Stoel, A.E.C., Gourvès, R., Bacconnet, C., et al., 2009. Essai de chargement de pointe: facteurs d'influence et détermination de modules de déformation. In: *Proceedings of the 17th International Conference on Soil Mechanics and Geotechnical Engineering*, vol. 2, pp. 985-988 (in French).
- Amar S., Baguelin, F., Canepa, Y., and Frank, R. (1994). Experimental study of the settlement of shallow foundations. Vertical and Horizontal Deformations of Foundations and Embankments, Vol. 2, GSP No. 40, ASCE, Reston, pp. 1602-1610.
- Arbaoui, H., Gourvès, R., Bressolette, P., Bodé, L., 2006. Mesure de la déformabilité des sols in situ à l'aide d'un essai de chargement statique d'une pointe pénétrométrique. *Can. Geotech. J.* 43, 355-369 (in French).
- Aussedat, G. 1970. "Sollicitations rapides des sols." *Thèse 3e cycle, Grenoble, 1970, France*.
- Balachowski, L., Kurek, N., 2008. Influence of boundary conditions in penetration testing. *Arch. Civ. Eng.* 54 (4), 653-668.
- Batilas, A., Pelekis, P.G., Roussos, P., Athanasopoulos, G.A., 2016. SPT energy measurements: manual vs. automatic hammer release. *Geotech. Geol. Eng.* 35, 879-888.

- Baudrillard, J. (1974). "New development in dynamic penetration testing." *Proceedings of 1st European symposium on penetration testing, Stockholm, Sweden*, 25–32.
- Be, Max Cope. 2011. "Dynamic Probe Theory Revisited – Effective Interpretation of Dynamic Test Results." In <http://www.docstoc.com/docs/77766375/DYNAMIC-PROBE-THEORYREVISITED>.
- Benz-Navarrete, M. A. (2009). *Mesures dynamiques lors du battage du penetromètre Panda 2*. [Phd dissertation]. Université Blaise Pascal.
- Benz Navarrete, M. A., Escobar Valencia, E. J., Gourvès, R., Haddani, Y., Breul, P., & Bacconnet, C. (2013). Mesures dynamiques lors du battage pénétrométrique – Détermination de la courbe charge-enfoncement dynamique en pointe. *Proceedings of the 18th International Conférence on Soil Mechanics and Geotechnical Engineering*, 499–502.
- Benz Navarrete, M., Breul, P., & Gourvès, R. (2021). Application of wave equation theory to improve dynamic cone penetration test for shallow soil characterisation. *Journal of Rock Mechanics and Geotechnical Engineering*. <https://doi.org/10.1016/j.jrmge.2021.07.004>
- Benz-Navarrete, M. A., Breul, P., & Arancibia, G. V. (2020). Correlation between static (CPT) and dynamic variable energy (Panda) cone penetration tests. *6th International Conference on Geotechnical and Geophysical Site Characterization*.
- Benz-Navarrete, M. A., Breul, P., & Gourvès, R. (2022). Application of wave equation theory to improve dynamic cone penetration test for shallow soil characterization. *Journal of Rock Mechanics and Geotechnical Engineering 14* 289-302.
- Broms, B., & Flodin, F. (1988). History of soil penetration testing. *Proceedings ISOPT1, Orlando, U.S.A., 1*, 157–220.
- Bussac, M.N., Collet, P., Gary, G., Othman, R., 2002. An optimisation method for separating and rebuilding one-dimensional dispersive waves from multi-point measurements. Application to elastic or viscoelastic bars. *J. Mech. Phys. Solid.* 50 (2), 321-349.
- Butcher, A. P., McElmeel, K., & Powell, J. J. M. (1996). Dynamic probing and its use in clay soils. In *Advances in site investigation practice* (pp. 383–395). <https://doi.org/10.1680/aisip.25134.0032>
- Butler, J., Caliendo, J., Goble, G.G., 1998 Comparison of SPT energy measurement methods. In: *Proceedings of the 1st International Conference on Site Characterization*, vol. 2, pp. 901e905.
- Byun, Y.H., Lee, J.S., 2013. Instrumented dynamic cone penetrometer corrected with transferred energy into a cone tip: a laboratory study. *Geotech. Test J.* 36 (4), 533-542.
- Casem, D.T., Fourney, W., Chang, P., 2003. Wave separation in viscoelastic pressure bar using single point measurements of strain and velocity. *Polym. Test.* 22 (2),155-164.
- Chaigneau, L. (2001). *Caracterisation des milieux granulaires de surface al'aide d'un penetrometre* [Phd dissertation]. Université Blaise Pascal.
- Chen, C., 1991. Energy Measurements during the Standard Penetration Test. *MS Thesis. University of Colorado, Boulder, Colorado, USA*.
- Chua, Koon Meng, and Robert L. Lytton. 1988. "Dynamic Analysis Using the Portable Pavement Dynamic Cone Penetrometer." *Transportation Research Record*, no. 1192. <http://trid.trb.org/view.aspx?id=302033>.
- Daniel, C., J. Howie, R. Jackson, and B. Walker. 2005. "Review of Standard Penetration Test Short Rod Corrections." *Journal of Geotechnical and Geoenvironmental Engineering* 131(4): 489-97. doi:10.1061/(ASCE)10900241(2005)131:4(89).
- Dahlberg, R. and Bergdahl, V. (1974). "Investigations of the swedish ramsounding method. *proc., european symposium on penetration testing.*" *European Symposium on Penetration Testing, Stockholm, Sweden*, 93–101.
- Eiksund, G., Nordal, S., 1996. Dynamic model pile testing with pore pressure measurements. *Proceedings of the 5th International Conference of Applied Stress- Wave Theory to Piles*, pp. 581-588.
- Emerson, Mark. 2005. "Corrélations entre données géotechniques et géophysiques à faible profondeur dans des sables." *Thèse de doctorat, Grenoble, France: Institut national polytechnique*.
- Escobar Valencia, E. J. (2015). *Mise au point et exploitation d'une nouvelle technique pour la reconnaissance des sols : le PANDA 3* [University of Clermont-Auvergne]. <https://tel.archives-ouvertes.fr/tel-01519486>
- Escobar Valencia, E.J., Benz Navarrete, M.A., Gourvès, R., Breul, P., 2013. Dynamic cone penetration tests in granular media: determination of the tip's dynamic load-penetration curve. In: *Proceedings of the 7th International Conference on Micromechanics*

- of *Granular Media*, vol. 1542, pp. 389-392. *Powder and Grains*.
- Escobar Valencia, E.J., Benz Navarrete, M.A., Gourvès, R., Breul, P., Chevalier, B., 2016a. In-situ determination of soil deformation modulus and the wave velocity parameters using the Panda 3 . In: *Proceedings of the 5th Geotechnical on Geotechnical and Geophysical Site Characterization (ISC'5)*, vol. 1, pp. 279-284.
- Escobar Valencia, E.J., Benz Navarrete, M.A., Gourvès, R., Haddani, Y., Breul, P., Chevalier, B., 2016b. Dynamic characterization of the supporting layers in railway tracks using the dynamic penetrometer Panda 3. *Procedia Eng* 143,1024-1033.
- Farrar, J. A. 1998. "Summary of Standard Penetration Test (SPT) Energy Measurement Experience." In *Proc. 1st Int. Conf. on Site Characterization, Atlanta*, 2:919-26.
- Farrar, J.A., Nickell, J., Allen, M.G., Goble, G.G., Berger, J., 1998. Energy loss in long rod penetration testing - terminus dam liquefaction investigation. In: *Proceedings of the ASCE Specialty Conference on Geotechnical Earthquake Engineering and Soil Dynamics III*, vol. 75, pp. 554-567.
- Foray, Pierre. 1972. "Contribution à l'étude des tassements et de la force portante des pieux." *Thèse de doctorat, Grenoble, France: Université Joseph Fourier*.
- Forestti Oliveira C., (2022). Interprétation de l'essai de chargement dynamique en pointe pénétrométrique, *PhD Thesis Clermont Auvergne University*.
- Frank, R. 1995. *Fondations Profondes*. Ed. Techniques Ingénieur.  
<https://books.google.fr/books?hl=fr&lr=&id=tKytGHzfQf4C&oi=fnd&pg=PA1&dq=Fondation+s+profondes+Roger+FRANK&ots=hAKHxCpRm&sig=BqiXW7rSHvB4srhUn8d1kiTzSfE>.
- Goble, G.G., Likins, G.E., Rausche, F., 1975. Bearing capacity of piles from dynamic measurements. *Case Western Reserve University, Cleveland, Ohio, USA. Technical Report No. OHIO-DOT-05-75*.
- Goble, G.G., Aboumatar, H., 1992. Determination of wave equation soil constants from the standar penetration test. In: *Proceedings of the 4th International Conference of Applied Stress-Wave Theory to Piles*, pp. 99-103.
- Goble, G.G., Aboumatar, H., 1994. Dynamic Measurements on Penetrometers for Determination of Foundation Design. University of Colorado, Boulder, Colorado, USA. *Technical Report No. CDOH-DTD-R-94-12*.
- Gonin, H., 1979. Réflexions sur le battage des pieux. *Rev. Fr. Geotech.* 9, 41-50 (in French).
- Goldmann, N. (1699). Comprehensive guidelines to the art of building (*Vollständige Anweisung zu der Civil Bau-Kunst*).
- Gourvès, R. (1991). *Le PANDA : pénétromètre dynamique léger à énergie variable pour la reconnaissance des sols*.
- Grésillon, Jean-Michel. 1970. "Etude des fondations profondes en milieu pulvérulent." *Thèse de doctorat, 1811-1970, France: Université de Grenoble. Faculté des sciences*.
- Holeyman, A., 1992. Technology of pile dynamic testing. In: *Proceedings of the 4th International Conference of Applied Stress-Wave Theory to Piles*, pp. 195-215.
- Hussein, M.H., Goble, G.G., 2004. A brief history of the application of stress-wave theory to piles. In: *Geotechnical Special Publication, vol. 125. American Society of Civil Engineers (ASCE)*, pp. 186-201.
- Isaacs, D.V., (1931). *Reinforced concrete pile formulae*. *J. Inst. Eng. Aust.* 12, 312-323.
- Iskander, M., Bless, S., Omidvar, M., 2015. Rapid Penetration into Granular Media: Visualizing the Fundamental Physics of Rapid Earth Penetration. *Elsevier*.
- ISO-22476-2. (2005a). *Reconnaissance et essais géotechniques — Essais en place — Partie 2: Essais de pénétration dynamique*.
- ISO-22476-2. (2005b). *Reconnaissance et essais géotechniques — Essais en place — Partie 2: Essais de pénétration dynamique*.
- Jara F., (2013), "Etude d'une nouvelle méthodologie pour la détermination du potentiel de liquéfaction des sols à l'aide du Panda 3® et de la géoendoscopie: Cas des «tranques de Relave» au Chili," *Master Thesis, Polytech' Clermont Ferrand, (in French)*.
- Jayawickrama, P. W., Amarasiri, A. L., & Regino, P. E. (2000). Use of dynamic cone penetrometer to control compaction of granular fill. *Transportation Research Record*, 1736, 71-80. <https://doi.org/10.3141/1736-10>
- Jung, B., Park, Y., Park, Y.S., 2006. Longitudinal acceleration wave decomposition in time domain with single point axial strain and acceleration measurements. In: *Proceedings of the 8th International Conference on Motion and Vibration Control. MOVIC 2006*, pp. 1-6.
- Kelevišius, K., Žaržojus, G., 2016. Initial DPSH soil test results with accelerometer installed in the probe cone. In: *Proceedings of the 13th Baltic Sea Region Geotechnical Conference*, pp. 118-121.

- Kianirad, E., Gamache, R., Brady, D., Alshawabkeh, A., 2011. *Equivalent quasi-static estimation of dynamic penetration force for near surface soil characterization*. In: Proceedings of Geo-Frontiers Congress 2011. American Society of Civil Engineers(ASCE), pp. 2325-2334.
- Kim, S. Y., Lee, J. S., Kim, D. J., and Byun, Y. H. (2021). Comparative study on estimation methods of dynamic resistance using dynamic cone penetrometer. *Sensors*, 21(9), 1–12.
- Larsson R. (2001) Investigations and Load Tests in Clay till Results from a series of investigations and load tests in the test field at Tornhill outside Lund in southern Sweden, Swedish Geotechnical Institute, Report No 59, 169 pages
- Liang, R.Y., Sheng, Y., 1993. Wave equation parameters from driven-rod test. *J. Geotech. Eng.* 119 (6), 1037-1057.
- Livneh, M., & Livneh, N. A. (2013). The use of the dynamic cone penetrometer for quality control of compaction operations. *International Journal of Engineering Research in Africa*, 10, 49–64. <https://doi.org/10.4028/www.scientific.net/JE/RA.10.49>
- Lodygowski, T., Rusinek, A., 2014. Constitutive Relations under Impact Loadings: Experiments, Theoretical and Numerical Aspects. *Springer, Heidelberg, Germany*.
- Lowery, L.L., Finley, J.R., Hirsch, T.J., 1968. *A comparison of dynamic pile driving formulas with the wave equation*. Texas Transportation Institute, Texas A&M University, Texas, USA. Technical Report No. 33-12.
- Luong, T. A., Denis, M., Reiffsteck, P., Benz-Navarrete, M., Maslač, J., Kordić, B., Hürtgen, J., Mathes-Schmidt, M., Koelzer, A., Josephine-Louis, K., Perrey, H., Spiekermann, C., Vosskuehler, L., Filjak, R., Belić, N., Budić, M., Baize, S. (2023). Use of the new dynamic cone penetrometer for the study of soil liquefaction along the Kupa river, Petrinja area. *9th Conference of Croatian Geotechnical Society, Geotehnika u epicentru – Petrinja 2020*, Sisak.
- Luong, T. A., Reiffsteck, P., Szymkiewicz, F., Navarrete, M., (2024a). Direct design method of shallow foundation based on in situ tests results, application to dynamic cone penetrometer. *Proceedings of the 18th ECSMGE, Lisbonne*,
- Luong T.A., Reiffsteck P. , Benz-Navarrete M., Szymkiewicz F., (2024b) In-situ experimental tests for shallow foundation design using dynamic penetration testing method, 7ISC
- Mayne P. W (2006). In-situ test calibration for evaluating soil parameters. In-situ testing. Singapore Workshop, p. 1-56.
- Middendorp, P., Weele, V., 1986. *Application of characteristic stress wave method in offshore practice*. In: Proceedings of the 3rd International Conference on Numerical Methods in Offshore Piling, vol. 1, pp. 6-18.
- Meunier, J., 1974. Contribution à l'étude des ondes et des ondes de choc dans les sols. *PhD Thesis. University of Grenoble, Grenoble, France (in French)*.
- Mohammadi, S. D., Nikudel, M. R., Rahimi, H., and Khamsehchiyan, M. (2012). "Unit skin friction from the extended dynamic cone penetrometer (edcp) test supplemented by measurement of torque within testing wells." *Iranian Journal of Science and Technology - Transactions of Civil Engineering*, 36(1), 115–119.
- Morgano, C. M., and R. Liang. 1992. "Energy Transfer in SPT-Rod Length Effect." *In International Conference on the application of stress-wave theory to piles*, 4:121–27.
- Nazarian, Soheil, Vivek Tandon, Kevin Crain, and Deren Yuan. 2000. "Use of Instrumented Dynamic Cone Penetrometer in Pavement Characterization." *ASTM Special Technical Publication 1375*: 214-30.
- Odebrecht, E., F. Schnaid, M. Rocha, and G. de Paula Bernardes. 2005. "Energy Efficiency for Standard Penetration Tests." *Journal of Geotechnical and Geoenvironmental Engineering* 131 (10): 1252–63. doi:10.1061/(ASCE)10900241(2005)131:10(1252).
- Omidvar, M., Iskander, M., Bless, S., 2014. Response of granular media to rapid penetration. *Int. J. Impact Eng.* 66, 60-82.
- Omidvar, M., Malioche, J.D., Bless, S., Iskander, M., 2015. Phenomenology of rapid projectile penetration into granular soils. *Int. J. Impact Eng.* 85, 146-160.
- Othman, R., 2014. Comparison of three methods to separate waves in the processing of long-time Hopkinson bar experiments. *Int. J. Mech. Eng. Technol.* 5, 114-119.
- Oularbi, A., 1989. Applicabilité des mesures dynamiques au calcul des pieux. *PhD Thesis. University of Nantes, Nantes, France (in French)*.
- Oularbi, A., Levacher, D., 2009. Réponse dynamique de la pointe d'un modèle de pieu dans un sol granulaire. In: *Proceedings of the Coastal and Maritime Mediterranean Conference, vol. 1, pp. 49-52*.
- Paikowsky, Samuel G., John E. Regan, and John J. McDonnell. 1994. *A Simplified Field Method*

- for the Capacity Evaluation of Driven Piles. Federal Highway Administration.
- Palacios, A., 1977. The Theory and Measurement of Energy Transfer during Standard Penetration Test Sampling. *PhD Thesis. University of Florida, Gainesville, USA.*
- Park, S.W., Zhou, M., 1999. Separation of elastic waves in split Hopkinson bars using one-point strain measurements. *Exp. Mech.* 39, 287-294.
- Puech, Alain. 1975. "De l'influence de la compressibilité sur la force portante limite des fondations profondes." *Thèse 3e cycle, Grenoble I, 1975, France.*
- Quezada, J.C., Breul, P., Saussine, G., Radjai, F., 2014. Penetration test in coarse granular material using contact dynamics method. *Comput. Geotech.* 55, 248-253.
- Rausche, F., (1970). Soil Response from Dynamic Analysis and Measurements on Piles. *PhD Thesis. Case Western Reserve University, Cleveland, USA.*
- Rausche, F., Goble, G.G., Likins, G.E., 1985. Dynamic determination of pile capacity. *J. Geotech. Eng.* 111 (3), 367-383.
- Rausche, F., Goble, G.G., Moses, F., 1971. A new testing procedure for axial pile strength. In: *Proceedings of Offshore Technology Conference, vol. 1, pp. 633-642.*
- Rausche, F., Moses, F., Goble, G.G., 1972. Soil resistance predictions from pile dynamics. *J. Soil Mech. Found Div.* 98 (9), 917-937.
- Reiffsteck, P., Bacconnet, C., Gourvès, R., Goddé, E., van de Graaf, H., 2008. Determination of elastic modulus from stress controlled cone penetration test. In: *Proceedings of the 3rd International Conference on Site Characterization, vol. 1. ISC'3, pp. 1135-1138.*
- Reiffsteck, P., Thorel, L., Bacconnet, C., Gourvès, R., van de Graaf, H., 2009. Measurements of soil deformation by means of cone penetrometer. *Soils Found.* 49 (3), 397-408.
- Retamales, S.L., Canou, J., & Dupla, J.C. (2020). Development of a liquefaction risk assessment methodology using an instrumented lightweight dynamic penetrometer: calibration chamber tests. In: *Proceedings of the 6th International Conference on Site Characterization, ISC'6, Budapest*
- Retamales, S. (2022). *Development of method for evaluation of liquefaction potential of sands based on a dynamic penetrometer.* PhD ENPC, 233 pages.
- Robertson, P.K., & Wride, C.E. (1998). Evaluating cyclic liquefaction potential using the cone penetration test. *Canadian Geotechnical Journal*, 35, 442-459.
- Saint-Venant, M. (1867). "Mémoire sur le choc longitudinal de deux barres élastiques de grosseurs et de matières semblables ou différentes, et sur la proportion de leur force vive qui est perdue pour la translation ultérieure; et généralement sur le mouvement longitudinal d'un système de deux ou plusieurs prismes élastiques." *Journal de mathématiques pures et appliquées*, 4(12), 237-376 (in French).
- Sadr Abadi H. H., (2016). *In-situ identification of liquefiable soils by cyclic static penetrometer : physical and numerical modelling, PhD thesis University of Grenoble Alpes.*
- Salgado, R., Loukidis, D., Abou-Jaoude, G., Zhang, Y., 2015. The role of soil stiffness non-linearity in 1D pile driving simulations. *Geotechnique* 65 (3), 169-187.
- Sanglerat, G. (1972). *The penetrometer and soil exploration. Developments in geotechnical engineering* (Elsevier, Ed.). Elsevier.
- Sastre Jurado, C. (2018). *Exploitation du signal pénétrométrique pour l'aide à l'obtention d'un modèle de terrain* [Phd Dissertation]. Université Clermont Auvergne.
- Sastre Jurado, C., Benz Navarrete, M. A., Gourvès, R., Breul, P., & Bacconnet, C. (2016). Automatic methodology to predict grain size class from dynamic penetration test using neural networks. *Proceedings of the 5th International Conference on Geotechnical and Geophysical Site Characterisation, ISC 2016*, 2, 1465-1470.
- Sastre Jurado, C., Breul, P., Benz Navarrete, M. A. & Bacconnet, C. (2020). Automatic soil identification from penetrometric signal by using artificial intelligence techniques; *Can. Geotech. J.* 58(8),1-11 (2020) [dx.doi.org/10.1139/cgj-2020-0422](https://doi.org/10.1139/cgj-2020-0422)
- Sastre Jurado, C., Breul, P., Bacconnet, C., & Benz Navarrete, M. A. (2021). Probabilistic 3D modelling of shallow soil spatial variability using dynamic cone penetrometer results and a geostatistical method. *Georisk*, 15(2), 139-151. <https://doi.org/10.1080/17499518.2020.1728558>
- Schmertmann, J. H., & Palacios, A. (1979). Energy Dynamics of SPT. *Journal of the Geotechnical Engineering Division*, 105(8), 909-926.
- Schnaid, F., Lourenço, D., & Odebrecht, E. (2017). Interpretation of static and dynamic penetration tests in coarse-grained soils. *Géotechnique Letters*, 7, 1-6. <https://doi.org/10.1680/jgele.16.00170>
- Schnaid, F., Odebrecht, E., & Rocha, M. (2007). On the mechanics of dynamic penetration tests.

- Geomechanics and Geoengineering*, 2, 137–146.  
<https://doi.org/10.1080/17486020701383825>
- Schnaid, F., Odebrecht, E., Rocha, M., & Bernardes, G. (2009). Prediction of Soil Properties from the Concepts of Energy Transfer in Dynamic Penetration Tests. *Journal of Geotechnical and Geoenvironmental Engineering*, 135. [https://doi.org/10.1061/\(ASCE\)GT.1943-5606.0000059](https://doi.org/10.1061/(ASCE)GT.1943-5606.0000059).
- Seed, H. B., & Idriss, I. M. (1971). Simplified Procedure for Evaluating Soil Liquefaction Potential. *Journal of the Soil Mechanics and Foundations Division*, pp 1249–1273.
- Seed, H. B., Tokimatsu, K., Harder, L. F., & Chung, R. M. (1985). Influence of SPT procedures in soil liquefaction resistance evaluations. *Journal of Geotechnical Engineering*, pp 1425–1445.
- Seed, R. B., & Harder, L. F. (1990). SPT-based analysis of cyclic pore pressure generation and undrained residual strength. In *H. Bolton Seed Memorial Symposium Proceedings (2)*, pp 351–376.
- Skempton, A.W., 1986. Standard penetration test procedures and the effects in sands of overburden pressure, relative density, particle size, ageing and overconsolidation. *Geotechnique* 36 (3), 425e447.
- Smith, E.A.L., 1960. Pile driving analysis by the wave equation. *J. Soil Mech. Found Div.* 86 (4), 35-61.
- Smith, E. A. 1962. "Pile-Driving Analysis by the Wave Equation." *American Society of Civil Engineers Transactions*.
- Sy, A., and Campanella R. G.. 1991. "An Alternative Method of Measuring SPT Energy." In *Proc., 2nd Int. Conf. on Recent Advances in Geotechnical Earthquake Engineering and Soil Dynamics*, 499–505. *Univ. of Missouri-Rolla*.
- Tatsunori M., Sekiguchi H., Yoshida H., and Kita K.. 1992. "Significance of Two-Point Strain Measurement in SPT." *Soils and Foundations* 32 (2):67–82.
- Terzaghi K., Peck R. (1948) *Soil Mechanics in Engineering Practice*, 1st edition, New York Wiley, 719 pages
- Tran, Q.A., Chevalier, B., Breul, P., 2016. *Discrete modeling of penetration tests in constant velocity constant velocity and impact conditions*. *Comput. Geotech.* 71, 12-18.
- Tran, Q.A., Benz Navarrete, M.A., Breul, P., Chevalier, B., Moustan, P., 2019. Soil dynamic stiffness and wave velocity measurement through dynamic cone penetrometer and wave analysis. In: *Proceedings of the 16th Pan-American Conference on Soil Mechanics and Geotechnical Engineering, vol. 1, pp. 401-408*.
- Tran, Q.A., Chevalier, B., Benz Navarrete, M.A., Breul, P., Gourvès, R., 2017. Modeling of light dynamic cone penetration test - panda 3 in granular material by using 3D Discrete element method. In: *Proceedings of the 8th International Conference on Micromechanics on Granular Media, vol. 140, pp. 1-4*.
- Verruijt, A., 2010. An Introduction to Soil Dynamics, 24th ed. *Springer, Dordrecht, the Netherlands*.
- Youd, T. L., Idriss, I. M., Andrus, R. D., Arango, I., Castro, G., Christian, J. T., Dobry, R., Finn, W.D.L., Harder, L F., Hynes, M.E., Ishihara, K., Koester, J.P., Liao, S.S.C., Marcuson, W.F., Martin, G.R., Mitchell, J.K., Moriwaki, Y., Power, M.S., Robertson, P.K., Seed, R.B., Stokoe, K. (2001). Liquefaction resistance of soils: Summary report from the 1996 NCEER and 1998 NCEER/NSF Workshops on Evaluation of Liquefaction Resistance of Soils. *J. Geotech. Geoenviron. Eng.* 127(10), pp 817-833
- Yu, H. S., and J. K. Mitchell. 1998. "Analysis of Cone Resistance: Review of Methods." *Journal of Geotechnical and Geoenvironmental Engineering* 124 (2): 140–49.
- Žaržojus, G., Kelevišius, K., Amšiejus, J., 2013. Energy transfer measuring in dynamic probing test in layered geological strata. *Procedia Eng* 57, 1302-1308.
- Zhao, H., Gary, G., 1997. A new method for the separation of waves. Application to the SHPB technique for an unlimited duration of measurement. *J. Mech. Phys. Solid.* 45 (7), 1185e1202.
- Zhang, N., Arroyo, M., Ciantia, M.O., Gens, A., Butlanska, J., 2019. Standard penetration testing in a virtual calibration chamber. *Comput. Geotech.* 111, 277-289.